Self-adjustment mechanism of bed structures under hydrology and sediment regimes

Huaixiang Liu, Zhaoyin Wang and Yongjun Lu

ABSTRACT

Bed structures develop in many coarse gravel-bed rivers, and the distribution of bed structures is obviously impacted by the environment conditions, especially hydrology and sediment regimes. This study carried out field investigations in natural tributaries of the Yangtze River to study the sizes of bed structures, their distribution in the basin, as well as their connections with local hydrology and sediment regimes. A field experiment was also conducted to study the evolution and functions of bed structures. Results of both the investigations and experiment indicated that under the conditions of low bedload, the structure intensity is in a positive correlation with the unit-width stream power, which is consumed by bed structures when the river is in a dynamic equilibrium. If the structures are not able to dissipate the whole energy, the river status turns into disequilibrium and the riverbed would be eroded by excess energy, and the river system would move to a stable position on the structure-power equilibrium line. The fluvial morphology of coarse-grained riverbeds is controlled by this mechanism to some extent. Sometimes excess energy can be consumed by bedload transport even with insufficient structure intensity, thus a unified power consumption model including bedload is also discussed.

Key words | bed structures, equilibrium, hydrology and sediment regimes, self-adjustment

Huaixiang Liu
Yongjun Lu (corresponding author)
State Key Laboratory of Hydrology-Water
    Resources and Hydraulic Engineering,
Nanjing Hydraulic Research Institute,
Nanjing 210029,
China
E-mail: yjlu@nhri.cn

Zhaoyin Wang
Department of Hydraulic and Hydropower
    Engineering,
Tsinghua University,
Beijing 100084,
China

INTRODUCTION

Riverbed configurations in natural streams are shaped by varying flows. On coarse-grained riverbeds, particles are usually moved to certain positions to form bed structures. Common bed structures include step-pool systems, ribbing structures, and boulder and cobble clusters (Wang & Lee 2008). (1) A step-pool system; Figure 1(a) is a geomorphologic phenomenon with alternating steps and pools and a stair-like appearance (Chin 1999; Wang *et al.* 2009). It usually develops in mountain streams of several meters width. Cobbles and boulders generally form the steps, which alternate with finer sediments in pools to produce a repetitive staircase-like longitudinal profile in the stream channel. (2) Figure 1(b) shows the Wasi River with ribbing structures. The Wasi River is a tributary of the Yangtze River in western China. In its channel, ribbing structures composed of cobbles, gravels, and some boulders have developed, extending out from the banks. (3) Figure 1(c) shows boulder clusters in the Wasi River. Boulder (or cobble) clusters are accumulations of sediments on either (or both) the lee or stoss side of an obstacle clast in rivers with poorly sorted sediments (Wittenberg 2002; Strom *et al.* 2006).

Bed structures have been observed in a wide range of both humid and arid environments (Chin 2002), and similar forms have even been found in glacial streams. Thus bed structures appear to be a fundamental element of relatively steep fluvial systems. There have been some studies on

Figure 1 | Common bed structures on coarse-grained riverbeds showing (a) step-pool, (b) ribbing and (c) boulder clusters.

common bed structures. Several variables are typically used to characterize micro-morphology of bed structures, including the mean structure height H, the mean structure length (distance between two individual structures) L (Figure 2), and so on. Researchers have used these variables to quantify bed structures and study the relations between these geometrical parameters and environmental conditions. Rosport (1997) reported that the length L of a regular step-pool system increases with the average flow discharge. Whittaker (1987) suggested that the length L of a regular step-pool system, or the distance between two steps or two pools, is inversely proportional to the average gradient of the stream $\bar{S}$:

$$L = 0.31\bar{S}^{-1.19} \tag{1}$$

where L is in meters. The decrease in L is rapid as the gradient increases up to about 0.15. The influence of the bed gradient on the adjustment of the step-pool morphology was further illustrated by a relation between the average step steepness (H/L) and the gradient obtained by Abrahams

et al. (1995) based on field and laboratory data:

$$S \le \frac{H}{L} \le 2S \tag{2}$$

This relation indicates that the average elevation loss due to steps is about 1 to 2 times as big as that due to the gradient. Experimental results of Wang *et al.* (2004) showed that the Manning's roughness coefficient n linearly increases with the scale of the bed structures.

Generally, bed structures are relatively stable under flow scouring and channel incision (Abrahams *et al.* 1995; Yu *et al.* 2008). They can reduce the lift and drag forces acting on the particles on the lee side of the structures (Reid 1992; Yang *et al.* 2006). Sear (1996) found that clusters on a gravel riverbed are usually very resistant to entrainment. The shear stress required to entrain clustered sediments is higher than that required to entrain dispersed bed particles (Hassan & Church 2000). Therefore, bed structures are sometimes used as stable habitats in ecological restoration projects (Yu *et al.* 2010, 2012a).

Some of the results cited above are mainly applicable locally due to restricted hydrology and sediment regimes. There were few past studies which could simulate the natural evolution process of bed structures due to limited conditions in the laboratory. A systematic study of bed structures is still required in order to reveal the essential mechanisms, which have been implied in previous valuable work. In order to analyze the distribution and evolution of bed structures under different conditions, as well as the underlying mechanism of fluvial morphology, several field investigations were carried out during this study and an
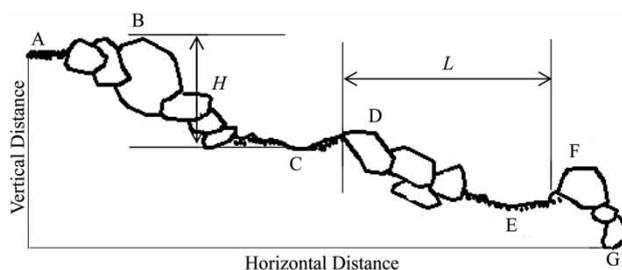
Figure 2 | A longitudinal profile of bed structures.

experiment was designed and conducted in a natural river valley.

METHODOLOGY

Field investigation in Diaoga River basin

The Diaoga River is a first-order headwater creek of the Xiaojiang River (a tributary of the Yangtze River, see Figure 3). It originates from the Huangcaoling Ridge (25 °56.078′N, 103°19.741′E, elevation 2,608 m), and joins the Xiaojiang River at Awang Town (25 °54.075′N, 103 °15.057′E, elevation 1,490 m), Yunnan Province, China. The Diaoga River falls 1,118 m in elevation within a distance of 12 km, resulting in an average gradient of 9.6%. The drainage area is approximately 54 km², 60.2% of which is farmlands.

The annual precipitation in the Diaoga River basin is about 1,000 mm, 2/3 of which concentrates during the flood season (June-September), leading to frequent rainstorms. The daily precipitation reached 35–55 mm on 2006/7/18, 2006/8/11, 2007/7/19 and 2007/8/11 during our investigation. Sometimes, flash floods or even debris flows occurred during these heavy storm events.

Frequent floods have caused the river basin to be incised by many ravines and gullies, most of which are located on the left bank (Figure 3). The Diaoga River basin was once covered by vast vegetation. However, in recent years, human activities including road construction, mining, and farm reclamation have severely destroyed the vegetation, resulting in intensive erosion and sediment-yielding in some gullies (mainly on the left bank).

Stable bed structures have developed in most river sections in the Diaoga River basin. Some structures, such as bedrock steps, boulder cascade (Figure 4) and large step-pools, are composed of very large stones, the size of which can reach up to 3–5 meters. As a comparison, some small bed structures, such as clusters, are categorized as 'Others'. Based on structure sizes from small to large, the structures described above can be categorized in the order of 'Others', 'Step-pools', 'Large step-pools', 'Boulder cascade/Bedrock steps'. Furthermore, the difference between the large and small structures is not just the stone size. For example, within the space of large step-pools, some sub-level step-pools or other small structures may also develop. During this investigation, the distribution of bed structures (size, type and GPS position) in the Diaoga River basin were all recorded.

Field experiment examining bed structures

The Jiangjiagou Ravine is another tributary of the Xiaojiang River (Figure 3). This ravine is known as a natural museum of debris flows. Over many years, the valley's bottom has been filled with layers of debris flow deposits. The poorly sorted deposits can provide various sediment resources (from clay to boulders) for the development of bed structures, forming an ideal place for the field experiment examining bed structure evolution and distribution. In this experiment, the surface of the deposits layer was assumed to be the original land surface without hydraulic erosion. Water and sediment were diverted onto the surface for river simulation so that free degradation, aggradation, and bed structures evolution could be observed.

On the deposit's surface, artificial shallow channels were pre-made for the water diversion from the Jiangjiagou main stream. The artificial channels were then reconnected to the main stream at their downstream exits (Figure 5). In the channel a small cement Parshall flume-type flow meter was made to estimate the discharge. An electronic theodolite was chosen to monitor the channel elevation change in both longitudinal and cross-sectional directions. Some other hydrological measurements were also taken during this experiment including the bedload transportation rate (measured by a sedimentation tank) and the grain size distribution (measured by the sieving method).

The experiment operation time was divided into three phases. For each phase, an artificial channel was pre-made at a different location (Table 1), and different hydrological schemes were adopted (Table 2). Two basic hydrological schemes, the bedload scheme (no treatment in the water and sediment diversion) and the non-bedload scheme (diverted bedload was removed by a sedimentation tank), were run alternatively. Each scheme started only after the previous scheme had reached a dynamic equilibrium. In order to simulate natural hydrological series, the diverted
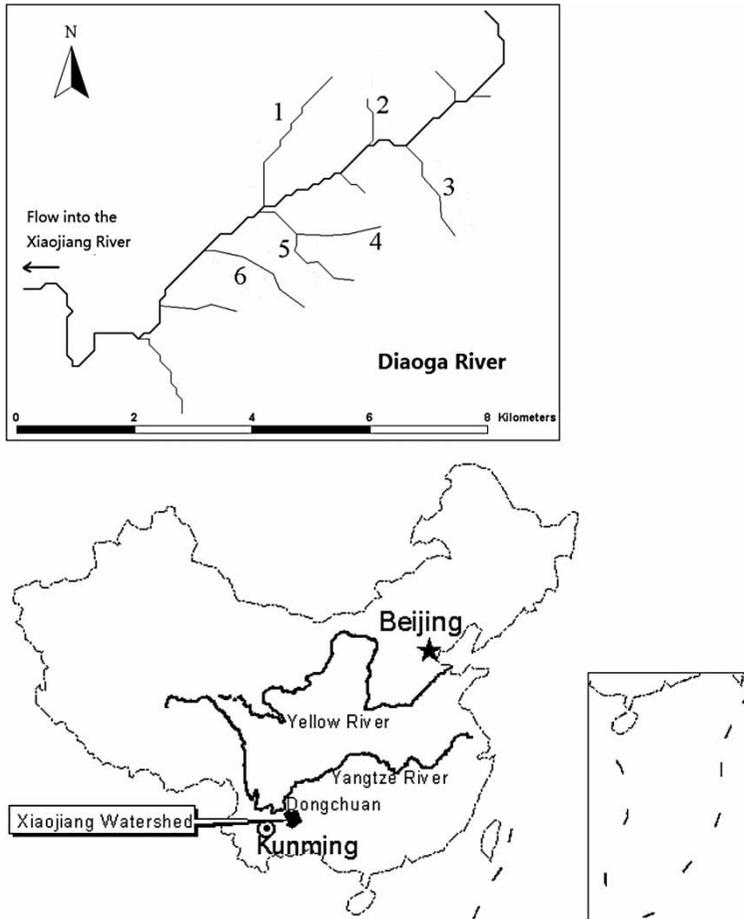
Figure 3 | River network and location of the Diaoga River. 1. Nianxiong Ravine; 2. Xunma Ravine; 3. Yincao Ravine; 4. Hetao Ravine; 5. Zhangjia Ravine; 6. Xiaoqiao Ravine.

discharge was controlled in alternating flood and low-water periods (Figure 6).
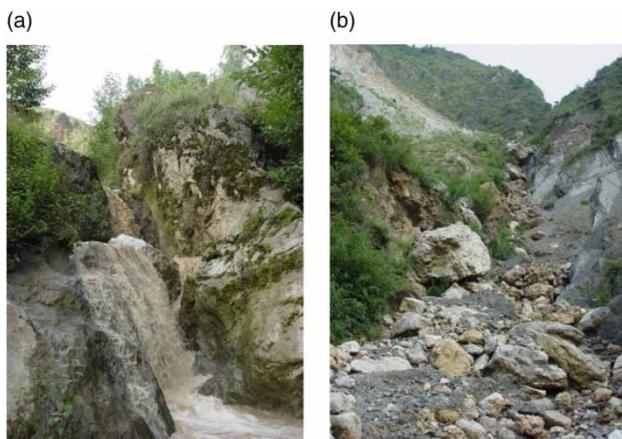
Figure 4 | Large-scale natural bed structures showing (a) bedrock steps and (b) boulder cascade.

The erosion base level was lower than the deposits surface by 1 to 1.5 m (cross-section AB in Figure 5). Thus in every phase the experiment started with severe retrogressive erosion. The channel incised rapidly and this effect gradually spread upward. After a period of bed evolution, bed structures evolved in certain arrangements and stabilized the channel, since coarse particles had remained and become structure components (Figure 7).

RESULTS

Field investigation in Diaoga River basin

The distribution of bed structures in the main stream and several large tributaries of the Diaoga River were recorded and summarized in Table 3. The river sections in the same
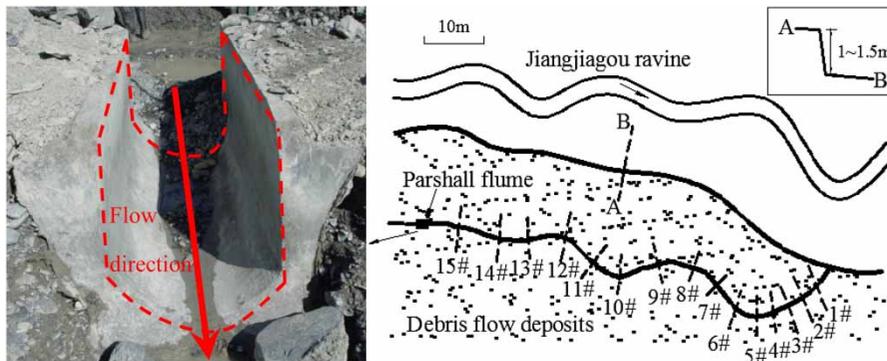
Figure 5 │ Layout of field experiment (phase 1).

ravine are numbered from upstream to downstream as A, B, C, etc. Channel gradients at the corresponding sections are also included in this table.

The statistics of the data in Table 3 are summarized in Table 4. It can be concluded that the sizes of bed structures increase as the channel gradient increases. Larger bed structures generally occur in higher gradient channels. After long-term fluvial morphology, most channels have adjusted to relatively stable conditions, which demonstrates that larger structures can protect the riverbed and in turn sustain channels with higher gradients. The only exception to this rule is the 'Others' structures in the river source, where high gradient (around 0.4) is paired with small grain size (D_{90}: 20 cm). Table 4 also shows that the type of structures have some influences. For example, the grain size of large step-pools and boulder cascade are similar (D_{90}: 50–150 cm), but the channel gradient they can sustain are very different (Large step-pools: 0.15–0.30, Boulder cascade: 0.30–0.50).

Bedload scheme in the experiment

The bedload scheme was run first in each phase (Table 2). The initial artificial channels were purposely made very

different (Table 1), but their longitudinal profiles in equilibrium status were almost identical under the same hydrological regime (Figure 8). Within the same reach, the formed bed structures were also quite similar among different phases (Table 5). These results demonstrate that the evolution and distribution of structures are in close relation to hydrological regimes. An increasing trend in the height and length of bed structures from upstream to downstream is shown in Table 5. The reason is that the particles remaining in the downstream riverbed after scouring were larger than those in the upstream (Figure 7). The downstream gradient is much steeper than that in the upstream (Table 5).

As for river patterns, all artificial channels became wandering rivers (Figure 9). Their main streams changed so frequently that the channel was widened to a shallow U-form and the width reached nearly 10 m.

Non-bedload scheme in the experiment

The non-bedload scheme was run after the bedload scheme in phase 2 and phase 3 (Table 2). The longitudinal profiles of channels after scouring of relatively clean water changed

Table 1 │ Initial geometric properties of artificial channels

Phase	Plan view	Cross-section	Channel depth (m)	Channel width (m)
1	Sinuous	U-shaped	0.5	1.0
2	Almost straight	V- shaped	1.0	0.8
3	Almost straight	U- shaped	0.3	1.0

Table 2 │ Basic process of field experiment

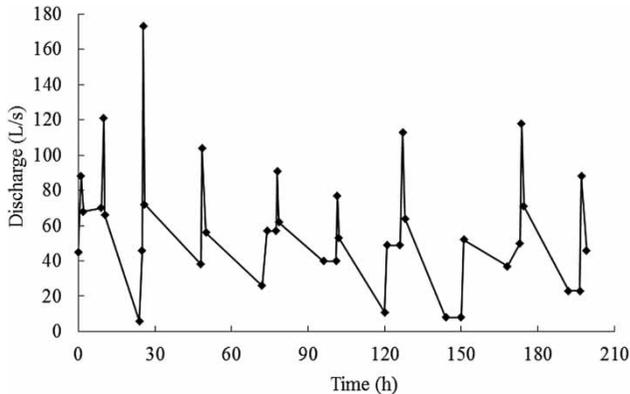| Phase	Hydrological scheme	Human intervention
1	Bedload scheme	No
2	Repeat phase 1, then non-bedload scheme	No
3	Repeat phase 2, then bedload scheme	Set artificial structures in middle reach during non-bedload scheme

Figure 6 | Discharge process.

significantly (Figure 8) due to severe incision. In phase 2, the thalweg elevation was lowered by 0.2 to 0.5 m compared to that for the bedload scheme. However, the channel's plane view seemed to be stationary (Figure 9). The channel stopped wandering and started to incise immediately after the bedload removal. Then the channel continued to get deeper and narrower and the previous sand bars along the banks became 'river terraces'.

The incision suggests that the bed structures, which formed in the bedload schemes, could not remain stable any longer. The incision depth in the upper reach was relatively large compared with that in the lower reach since the structures previously formed in the upstream reach were weaker (Table 6). Thus, the structures were strengthened especially in the upper reach. Then the structures in the upper and lower reaches became almost the same (Table 6) after the non-bedload scheme was completed.
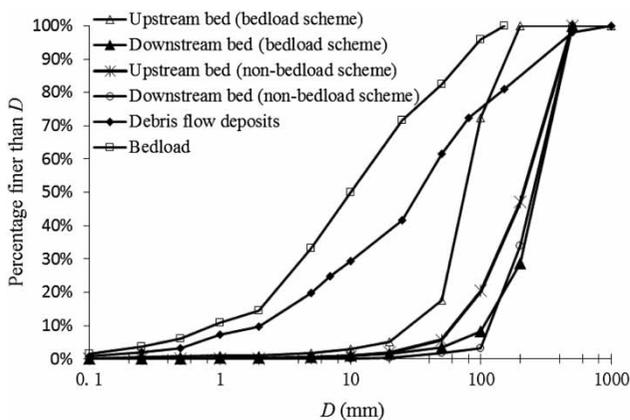

Figure 7 | Grain size distribution (Meral 2016) of deposits, bedload, and bed structures.

The structure variation also led to the adjustment of the corresponding channel gradient.

Artificial bed structures in the experiment

The non-bedload scheme in phase 3 was influenced by human interventions (Table 7). After the previous bedload scheme, artificial step-pool structures (height = 10 cm and length = 50 cm) were placed in the middle reach. Compared with phase 2, a full-scale incision was impeded (Figure 8) and only the upper reach was slightly eroded.

DISCUSSION

Preliminary analysis

The results of both field investigations and experiments have indicated that, larger bed structures can protect the riverbed of channels with higher gradient by sustaining relative stability. It means that the erosive energy is dissipated by the structures and can no longer destroy the riverbed. Thus a close numerical connection must exist between the bed structures and the erosive energy they consumed.

The effect of the river width was ignored by using the unit-width discharge q and stream gradient s to calculate the unit-width stream power p as the energy of water:

$$p = \gamma qs \tag{3}$$

The 'scale' of bed structures, however, is much more difficult to define precisely and quantitatively. As discovered in our field work, the commonly used variables such as the structure height H and the structure length L varied in a wide range (Tables 5–7), and their measurements were very subjective especially when the bed was not that regular. Another possible good choice for the description of bed structures is the grain size. Thus, an analysis of the field investigation results from the Diaoga River basin was done as follows. (1) Hydrology data were collected in 2006 and 2007 at a cross-section about 8.4 km downstream from the origin of main stream, and then the bankfull discharge could be estimated (it is believed that the

Table 3 | Distribution of bed structures in Diaoga River basin

River Name	Sections[a]	Gradient	Bed structures	Grain size/cm D_{90}	D_{10}	Perennial flow or not
Xiaoqiao Ravine	A	0.422	Others	20	<1	N
	B	0.297	Mostly bedrock steps	–	–	N
	C	0.399	Bedrock steps	–	–	Y
	D	0.344	Boulder cascade	150	20	Y
	E	0.164	Large step-pools	50	5	Y
	F	0.097	Others	20	1	Y
Hetao Ravine	A	0.388	Boulder cascade	100	20	N
	B	0.417	Boulder cascade, partly bedrock steps	100	20	Y
	C	0.160	Large step-pools	100	10	Y
	D	0.282	Mainly large step-pools, partly bedrock steps	100	10	Y
	E	0.336	Bedrock steps	–	–	Y
Zhangjia Ravine	A	0.380	Others	20	<1	N
	B	0.218	Step-pools, artificial check dams	20	5	Y
	C	0.206	Step-pools, artificial check dams	20	5	Y
	D	0.211	Step-pools, artificial check dams	20	5	Y
	E	0.399	Boulder cascade	150	50	Y
	F	0.124	Others	50	10	Y
	G	0.421	Bedrock steps	–	–	Y
	H	0.095	Others	20	1	Y
Yincao Ravine	A	0.483	Boulder cascade	150	20	N
	B	0.212	Step-pools, a little bedrock exposure	50	5	Y
	C	0.105	Step-pools	20	2	Y
Diaoga River (main stream)	A	0.313	Boulder cascade	50	10	Y
	B	0.075	Others	20	1	Y
	C	0.507	Bedrock steps	–	–	Y
	D	0.112	Others	10	1	Y
	E	0.121	Step-pools	50	5	Y
	F	0.044	Others	20	2	Y
	G	0.130	Step-pools	50	10	Y
	H	0.161	Large step-pools	150	20	Y
	I	0.116	Step-pools	50	10	Y
	J	0.066	Others	50	5	Y
	K	0.042	Others	50	5	Y
	L	0.068	Others	50	5	Y

[a]From upstream to downstream: river sections are labeled A, B, C onwards.

bankfull discharge is the most effective factor for creating the riverbed form). (2) The discharge of every river section (Table 3) was calculated using linear interpolation method, assuming that the river source discharge was 0, and then the stream power p could be obtained. A positive correlation between p and D_{50} is shown in Figure 10; however, the

Table 4 | Statistics of structures types, composition and channel gradient

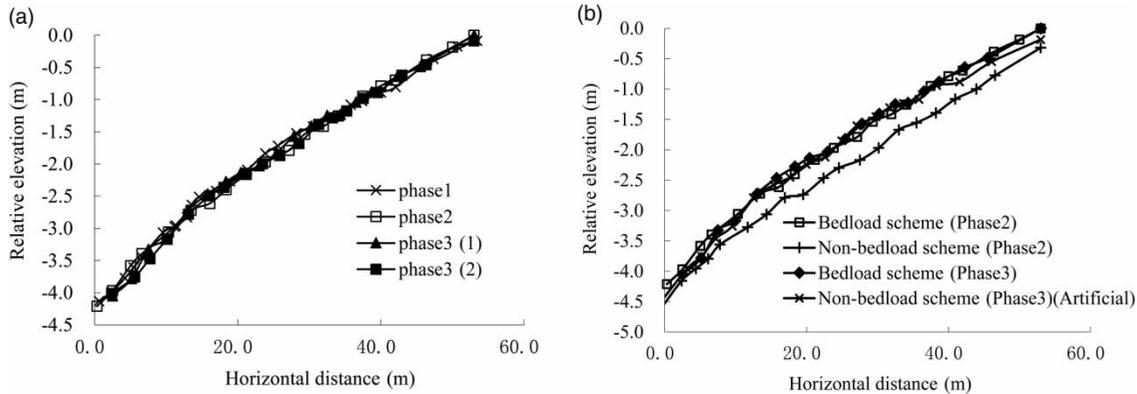| Bed structures	Others	Step-pools	Large step-pools	Bedrock steps	Boulder cascade	Others (in river source)
Channel gradient	<0.15	0.10–0.20	0.15–0.30	>0.30	0.30–0.50	Around 0.4
D_{90}/cm	10–50	20–50	50–150	–	50–150	20
D_{10}/cm	1–10	2–10	5–20	–	10–50	<1

Figure 8 | Equilibrium profile in the experiment for (a) bedload scheme and (b) non-bedload scheme.

data were very sparse since too many estimation methods were used. Further, as noticed in Table 4, grain size is not the only factor and the type of structures also has influences.

In this study, a new variable of bed structures scale was applied to avoid the defects mentioned above. Given a measured river profile (see Figure 2), a geometrical parameter S_p (called 'structure intensity' here) is defined as the 'curve length/straight length' ratio:

$$S_P = \frac{(AB + BCD + DEF + FG)}{\overline{AG}} - 1 \tag{4}$$

It is obvious that the parameter S_p can directly describe the coarseness of riverbed and the structure scale to some extent. For a smooth bed without any bed structures, the value of S_p is 0. Higher S_p values represent rougher riverbeds and larger scales of structures. For a given river profile, the value of S_p is unique and operator-independent, which is a better choice than common variables such as H, L and D_{50}.

In order to calculate the structure intensity, an instrument (Figure 11) was designed to measure the profile curve of riverbed (Wang & Lee 2008). In this instrument, parallel measuring rods placed on an aluminum steel frame can slide freely down onto the bed surface. The upper ends of the rods describe the bed profile in front of a screen when the frame is strictly adjusted to a horizontal position. A long river profile can be measured by moving the frame along the stream and taking continuous photos of the screen. The space between two rods is set to 5 cm, which is small enough to record any type of bed structures.

Equilibrium of structures and stream power

In the field experiments, the bedload played an important role in the evolution and distribution of structures. Therefore, we measured some river sections where the bedload transportation rates were not very high (so that the effect of bedload movement could be neglected). Their streambed intensity S_p and unit-width stream power p are shown in

Table 5 | Bed structures and channel gradients in bedload scheme

	Phase 1				Phase 2				Phase 3(1)	Phase 3(2)
		Structures				**Structures**				
Reach	**Channel gradient**	**Type**	**Height (cm)**	**Length (cm)**	**Channel gradient**	**Type**	**Height (cm)**	**Length (cm)**	**Channel gradient**	**Channel gradient**
Lower	0.110	S-P	8–15	70–150	0.100	S-P	6–13	30–170	0.110	0.100
Middle	0.072	S-P	Transition	Transition	0.079	S-P	Transition	Transition	0.074	0.075
Upper	0.061	S-P	3–5	40–70	0.065	S-P	3–6	30–70	0.063	0.060

Note: S-P is step-pool; 'Transition' means that structures of both upper and lower reaches exist.
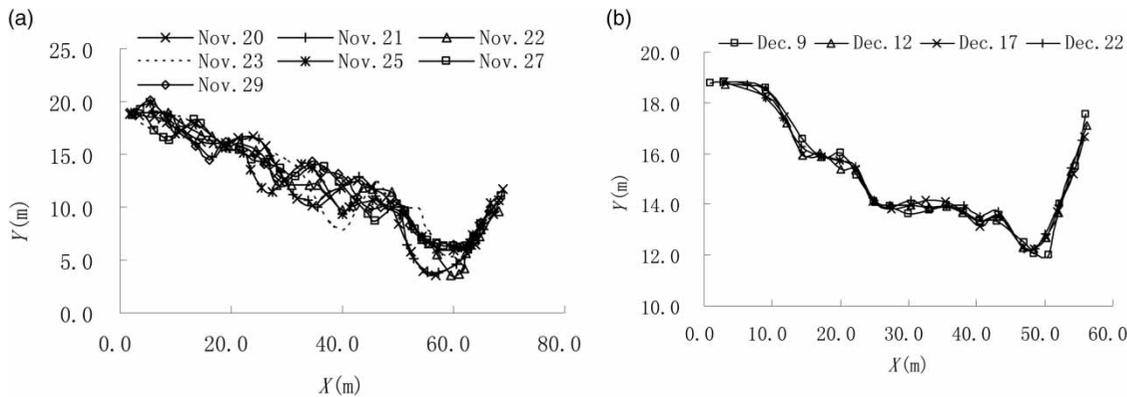
Figure 9 │ Planar channel wandering in the experiment for (a) bedload scheme and (b) non-bedload scheme.

Figure 12. Data from some natural rivers (mainly tributaries of the Yangtze River) and results of the field experiment (non-bedload scheme) are included on the plot. The diagram shows that a straight line can describe the positive correlation between S_p and p. Its function Equation (5) represents how much energy can be consumed by certain bed structure intensities.

$$p = p_0 S_p^{1.786}, p_0 = 6729 kg/s^3 \tag{5}$$

Figure 12 is also an equilibrium line, which reflects the distribution of structure intensity and stream power under dynamic equilibrium status. When a river section's status dot is located on (or above) this equilibrium line, the bed structures can consume all the erosive stream power and maintain the riverbed stability. However, when the status dot falls under the line, it means that the structure intensity is insufficient to protect the bed, so that excessive power will scour the bed. The transition from the bedload scheme to the non-bedload scheme (phase 2) in the field experiment is shown in Figure 13. At first, the status dots of the river sections were below the equilibrium line. Therefore, the riverbeds could not maintain its stability and erosion occurred immediately. With the channel incision, the structure intensity and channel gradient both changed, resulting in shifting of the dots on the diagram. Finally, the equilibrium between the structures and stream power was reached, the bed became stable and the dots stopped moving near the straight line. This mechanism also explained the exception in the Diaoga River basin (Table 4), i.e. small bed structures (marked as 'Others (in river source)') developed in high-gradient channels of some river source zones. This phenomenon only occurs in the Zhangjia Ravine and Xiaoqiao Ravine (Table 3). According to the field investigations, these two ravines are the most intensive sediment-yielding tributaries in the entire Diaoga River basin. The unbalance between the structures and stream power resulted in disequilibrium and severe erosion, then the sediment was transported and deposited downstream as thick flat layers near the mouths of the two tributaries.

Table 6 │ Comparison of bed structures and channel gradient of two schemes (phase 2)

	Bedload scheme				Non-bedload scheme			
		Structures				Structures		
Reach	Channel gradient	Type	Height (cm)	Length (cm)	Channel gradient	Type	Height (cm)	Length (cm)
Lower	0.100	S-P	6–13	30–170	0.083	S-P	6–12	70–100
Middle	0.079	S-P	Transition	Transition	0.072	S-P, R, C	6–9	100–200
Upper	0.065	S-P	3–6	30–70	0.072	S-P, R, C	7–10	100–200

Note: R is ribbing and C is cluster.

Table 7 │ Effect of artificial bed structures

Reach	Without artificial structures (phase 2)				Artificial structures (phase 3)			
		Structures				Structures		
	Channel gradient	Type	Height (cm)	Length (cm)	Channel gradient	Type	Height (cm)	Length (cm)
Lower	0.083	S-P	6–12	70–100	0.100	S-P	6–14	80–200
Middle	0.072	S-P, R, C	6–9	100–200	0.080	S-P, R	7–10	50–150
Upper	0.072	S-P, R, C	7–10	100–200	0.055	R, C	3–8	40–130

In fluvial morphology, long-term adjustment of flow and riverbed generally approaches equilibrium and stability. The balance between the structures and stream power should be satisfied when the river condition is near equilibrium and the bedload can be ignored. Thus, according to the analysis above, the development of bed structures are the results of riverbed adapting to the local hydrological regimes. If the structures are not well developed (not enough to dissipate all the energy), disequilibrium will occur and cause the riverbed to scour.

Consideration of bedload

The immediate incision (Figure 8) after the transition from the bedload scheme to the non-bedload scheme in the field experiment indicates that if there is enough bedload, the riverbed can still be protected even when the existing structures cannot consume all the energy (Figure 13). In other words, a proportion of the stream power was consumed by bedload. Thus, the removal of bedload will lead to imbalance and the excessive power will erode the bed to generate new bedload. The concept that the movement of bedload will increase energy loss has also been reported elsewhere (Song & Chiew 1997; Wang & Zhang 2012; Yu *et al.* 2012b). Therefore, for a river section where structures and massive bedload transportation both exist, the total loss of stream power p should be expressed as the sum of these two parts.

Based on Equation (5), which was derived under a condition with little bedload, the unified formula of energy consumption can be assumed in the form of Equation (6).

$$\frac{p}{p_0} = S_p^{1.786} + f\left(\frac{g_b g}{p_0}\right) \tag{6}$$

In this equation, f is still an unknown function, g_b is the unit-width bedload transportation rate (kg/m/s), and g is the gravitational acceleration (9.8 m/s^2). All three terms are
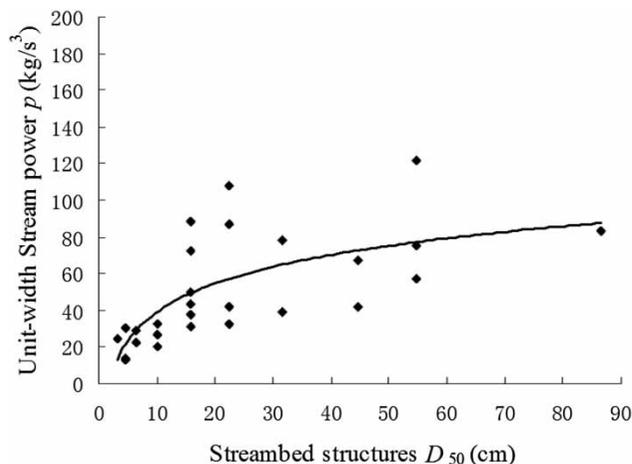
Figure 10 │ Diagram of stream power versus grain size of structures.
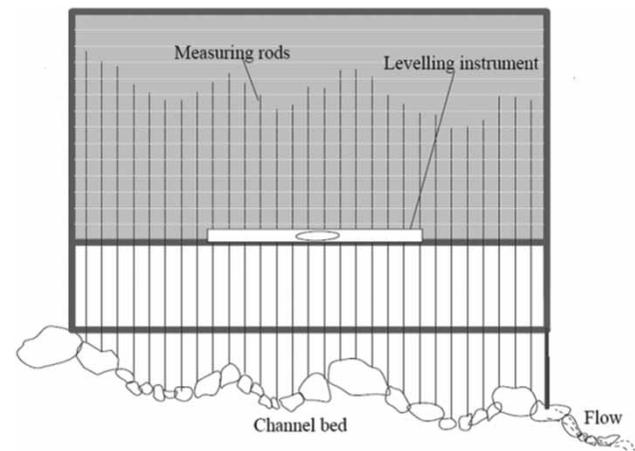
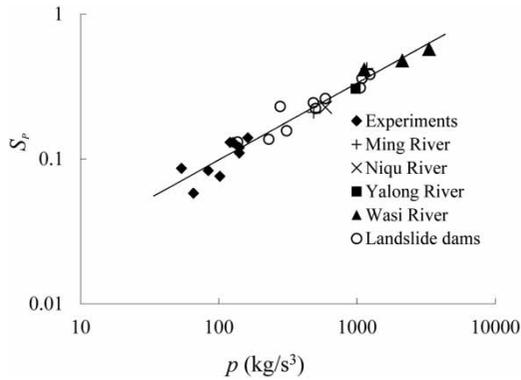**Figure 11** │ The instrument for riverbed profile measurement.

Figure 12 │ Equilibrium line of structure intensity and stream power.

Figure 14 │ The fitting of bedload-dissipation function f.

dimensionless (which is more scientific and reasonable), and they represent the total energy loss, structures-dissipation and bedload-dissipation. Yu (2008) conducted an experiment and measured S_p and g_b under a fixed value of stream power p. According to these data, we developed Figure 14 and Equation (7).

$$\frac{p}{p_0} = S_p^{1.786} + 0.027\left(\frac{g_b g}{p_0}\right)^{0.134} \tag{7}$$

Therefore, the form of Equation (6) is reasonable. However, due to the lack of data and the uncertainty of bedload rate measurement, Equation (7) is just a rough estimate in this study. The function f should be determined and verified carefully after further similar experiments.

Very few existing fluvial morphology models are bed structure-oriented, and most existing models are related to suspended load and large rivers. However, the mechanism
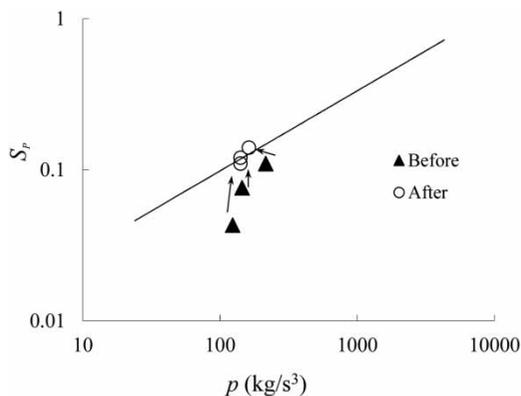
in this study is still related to these existing models. For example, similar to S_p, the Manning's roughness coefficient n and the Darcy-Weisbach coefficient f_d were frequently used to describe the bed effect against erosion in the existing models:

$$U = \frac{R^{2/3}s^{1/2}}{n} \tag{8}$$

$$U = \left(\frac{8gRs}{f_d}\right)^{1/2} \tag{9}$$

where U is the flow velocity in the river and R is the hydraulic radius. Based on several test runs in the field experiment, Figure 15 was given. It can be seen in Figure 15 that both n and f_d show similar tendencies since they are both related to a physical phenomenon – the bed resistance. However,
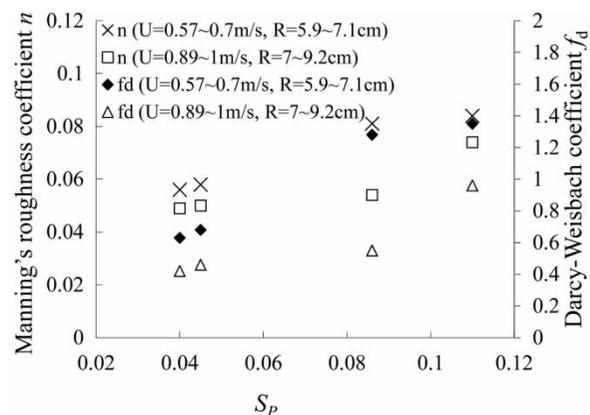

Figure 13 │ Status transition due to deficiency of structure intensity.

Figure 15 │ Structure intensity and resistance factors of existing models.

different from the pure geometry parameter S_p, the values of n and f_d may vary with the hydrological regime.

In general, the total bed resistance (such as n, f_d) can be divided into two parts: the grain resistance and the form resistance (i.e. S_p in this study). In the field experiment, in the river channels where bed structures developed, the bed became so rough that the form resistance remained in domination. Therefore, S_p shows a strong influence on n and f_d in Figure 15.

Therefore, the mechanism that has been discussed by this study can also be partly described by some existing models via this relationship. For instance, Wang et al. (1998) proposed a bed transformation model based on bedload:

$$-\frac{dZ}{dt} = \frac{g_{b*} - g_b}{I_b} \tag{10}$$

in which $-dZ/dt$ is the bed erosion rate (elevation decline), I_b is called the 'river bed inertia' (more stable beds tend to have higher inertia values), g_b is the actual bedload transport rate, and g_{b*} is the required bedload transport rate to reach equilibrium:

$$\left(\frac{\gamma}{g}\right)^{1/3}\left(\frac{\gamma_s - \gamma}{\gamma_s}\right)^{2/3} g_{b*}^{2/3} = 4\gamma Rs\left(\frac{K_b}{K'_b}\right)^{3/2} - 0.188(\gamma_s - \gamma)D_{50} \tag{11}$$

where K_b/K'_b is considered to be the grain resistance/total bed resistance (grain resistance + form resistance). In general,

$$\frac{K_b}{K'_b} \propto \frac{D_{90}^{1/6}}{n} \tag{12}$$

Therefore, the adjustment mechanism in our field experiment can be explained by this model: (1) in the bedload scheme, $g_b = g_{b*}$ so that $dZ/dt = 0$ (Equation (10)) and the bed was 'protected' by the bedload and was in equilibrium; (2) when the bedload from upstream was reduced, $g_b < g_{b*}$ so that $dZ/dt > 0$ and the channel started to incise; (3) during incision, the bed structure intensity S_p was enhanced, which in turn resulted in the increase of roughness n (Figure 15), while the bed composition (D_{90} and D_{50}) did not have significant change since most large boulders remained in place. I_b also increased due to the more stable bed. Thus, g_{b*} became smaller (Equation (11)) and the incision rate dZ/dt gradually slowed down.

CONCLUSIONS

Based on field work in several natural rivers and field experiments, bed structures and some of their essential principles were studied in this paper.

The evolution and distribution of structures was found to be in close relation to the hydrological conditions. The underlying principles were concluded to be: the stream power of a river section is consumed by both bed structures developed on the riverbed and bedload movement. A possible formula was derived, however further studies are still required to improve this unified energy theory, which could be an important mechanism in the research of mobile riverbed and fluvial morphology.

If the bedload can be neglected, then the channel will be stable when the equilibrium between the bed structures and stream power is reached. This means that the structures can dissipate all the erosive energy and protect the bed at this moment. A parameter called the structure intensity was defined and proven to quantify this relation well. When the structure intensity is not large enough, disequilibrium occurs and the excessive power will erode the riverbed. Generally, the river will re-adjust and new equilibrium will be reached. Therefore, the evolution of bed structures is in fact a process of the riverbed adapting to the local hydrological regimes. The fluvial morphology of streams with very coarse-grained riverbed is controlled by the dynamic process explained above.

ACKNOWLEDGEMENTS

REFERENCES

Abrahams, A. D., Li, G. & Atkinson, J. F. 1995 Step-pool stream: adjustment to maximum flow resistance. *Water Resources Research* **31**, 2593–2602.

Chin, A. 1999 The morphologic structure of step-pools in mountain streams. *Geomorphology* **127**, 191–204.

Chin, A. 2002 The periodic nature of step-pool mountain streams. *American Journal of Science* **302**, 144–167.

Hassan, M. A. & Church, M. 2000 Experiments on surface structure and partial sediment transport on a gravel bed. *Water Resources Research* **36**, 1885–1895.

Meral, R. 2016 A study on the estimating of sediment concentration with turbidity and acoustic backscatter signal for different sediment sizes. *Hydrology Research* **47**, 305–311.

Reid, J. B. 1992 The Owens River as a tiltmeter for Long Valley Caldera, California. *The Journal of Geology* **100**, 353–363.

Rosport, M. 1997 Hydraulics of steep mountain streams. *International Journal of Sediment Research* **12**, 99–108.

Sear, D. A. 1996 Sediment transport processes in riffle-pool sequences. *Earth Surface Processes and Landforms* **21**, 241–262.

Song, V. & Chiew, Y. M. 1997 Effect of bed-load movement on flow resistace. In: *Proceedings of the 27th Congress of the IAHR*, San Francisco, CA, pp. 1233–1238.

Strom, K. B., Papanicolaou, A. N., Billing, B., Ely, L. L. & Hendricks, R. R. 2006 Characterization of particle cluster bedforms in a mountain stream. In: *Proceedings of World Water and Environmental Resources Congress 2005*, American Society of Civil Engineers, Anchorage.

Wang, Z. Y. & Lee, H. W. 2008 *Integrated River Management*. Tsinghua University, Beijing, and the University of Hong Kong.

Wang, Z. Y. & Zhang, K. 2012 Principle of equivalency of bed structures and bed load motion. *International Journal of Sediment Research* **27**, 288–305.

Wang, Z. Y., Xu, Y. N. & Su, X. B. 1998 A study on channel scour rate of sediment laden flow and river bed inertia. *Journal of Sediment Research* **2**, 1–9 (in Chinese).

Wang, Z. Y., Xu, J. & Li, C. Z. 2004 Development of step-pool sequence and its effects in resistance and stream bed stability. *International Journal of Sediment Research* **19**, 161–171.

Wang, Z. Y., Melching, C. S., Duan, X. H. & Yu, G. A. 2009 Ecological and hydraulic studies of step-pool systems. *Journal of Hydraulic Engineering* **135**, 705–717.

Whittaker, J. G. 1987 Sediment transport in step-pool streams. In: *Sediment Transport in Gravel-Bed Rivers* (C. R. Thorne, J. C. Bathurst & R. D. Hey, eds). Wiley, Chichester, pp. 545–579.

Wittenberg, L. 2002 Structural Patterns and Bed Stability of Humid Temperate, Mediterranean and Semi-arid Gravel Bed Rivers. Ph.D. Dissertation. Newcastle University, Tyne and Wear, UK.

Yang, S. F., Hu, J. & Wang, X. K. 2006 Incipient motion of coarse particles in high gradient rivers. *International Journal of Sediment Research* **21**, 220–229.

Yu, G. A. 2008 Experimental Study on Bed Structures and Bedload Transport in an Incised Stream. Tsinghua University, Beijing.

Yu, G. A., Wang, Z. Y., Zhang, K. & Liu, H. X. 2008 Field experiment for harnessing incised mountain stream (the Diaoga River) by using artificial step-pools. *Journal of Hydroelectric Engineering* **27**, 85–89 (in Chinese).

Yu, G. A., Wang, Z. Y., Zhang, K., Duan, X. H. & Chang, T. C. 2010 Restoration of an incised mountain stream using artificial step-pool system. *Journal of Hydraulic Research* **48**, 178–187.

Yu, G. A., Huang, H. Q., Wang, Z. Y., Brierley, G. & Zhang, K. 2012a Rehabilitation of a debris-flow prone mountain stream in southwestern China – Strategies, effects and implications. *Journal of Hydrology* **414–415**, 231–243.

Yu, G. A., Wang, Z. Y., Huang, H. Q., Liu, H. X., Blue, B. & Zhang, K. 2012b Bed load transport under different streambed conditions – a field experimental study in a mountain stream. *International Journal of Sediment Research* **27**, 426–438.